Synthetic FLAIR as a Substitute for FLAIR Sequence in Acute Ischemic Stroke

Joseph Benzakoun, Marc-Antoine Deslys, Laurence Legrand, Ghazi Hmeydia, Guillaume Turc, Wagih Ben Hassen, Sylvain Charron, Clément Debacker, Olivier Naggara, Jean-Claude Baron, et al.

Synthetic FLAIR as a substitute for FLAIR sequence in acute ischemic stroke

Journal:	*Radiology*
Manuscript ID	RAD-21-1394.R2
Manuscript Type:	Original Research
Manuscript Categorization Terms:	MR-Imaging < 2. MODALITIES/TECHNIQUES, CNS < 4. AREAS/SYSTEMS, Brain/Brain Stem < 5. STRUCTURES, Comparative Studies < 7. METHODOLOGY

Synthetic FLAIR as a substitute for FLAIR sequence in acute ischemic stroke

Joseph Benzakoun, MD, MSc; Marc-Antoine Deslys, MSc; Laurence Legrand, MD, MSc; Ghazi Hmeydia, MD; Guillaume Turc, MD, PhD; Wagih Ben Hassen, MD, MSc; Sylvain Charron, PhD; Clément Debacker, PhD; Olivier Naggara, MD, PhD; Jean-Claude Baron, MD, ScD; Bertrand Thirion, PhD; Catherine Oppenheim, MD, PhD

From Department of Neuroradiology (J.B., L.L., G.H., W.B.H., O.N., C.O.), Department of Neurology (G.T., J.C.B.), GHU Paris Psychiatrie et Neurosciences, Paris, France; INSERM U1266 (J.B., M.A.D., L.L., G.T., W.B.H., S.C., C.D., O.N., J.C.B, C.O.), Paris, France; Université de Paris, FHU Neurovasc (J.B., L.L., G.T., W.B.H., S.C., C.D., O.N., J.C.B., C.O.), Paris, France; and PARIETAL team (B.T.), INRIA, Saclay, France

Corresponding author:

Joseph Benzakoun, Department of Neuroradiology, GHU Paris Psychiatrie et Neurosciences, Site Sainte-Anne, 1, rue Cabanis, 75014 Paris, France.

Email benzakoun.joseph@gmail.com; Phone +33145657710

Funding: None

Manuscript type: Original research

Word count: 2805

Abbreviated Title Page

Synthetic FLAIR as a substitute for FLAIR sequence in acute ischemic stroke

Manuscript type: Original research

Summary statement

Synthetic fluid-attenuated inversion recovery (FLAIR) generated with deep learning is as accurate as a real FLAIR sequence for the identification of early stroke.

Abbreviations:

AIS = acute ischemic stroke

DWI = diffusion-weighted imaging

FLAIR = fluid-attenuated inversion recovery

GAN = Generative Adversarial Network

rSI = relative signal intensity

WMH = white matter hyperintensities

Key results

- Synthetic fluid-attenuated inversion recovery (FLAIR) can be generated from a diffusion-weighted imaging (DWI) sequence using deep learning within 22 seconds.
- The diagnostic performance of synthetic FLAIR to identify early (≤4.5hrs) ischemic stroke was similar to that of real FLAIR (sensitivity and specificity: 85% and 92% vs. 82% and 92%, respectively).
- Use of synthetic FLAIR instead of real FLAIR may allow a clinically relevant (≈25%) reduction in stroke MR protocol duration.

Abstract

Background: In acute ischemic stroke (AIS), fluid-attenuated inversion recovery (FLAIR) is used for treatment decision when onset time is unknown. Synthetic FLAIR could be generated with deep learning from information embedded in diffusion-weighted imaging (DWI) and replace real FLAIR to shorten MRI acquisition.

Purpose: To compare performance of synthetic and real FLAIR for DWI-FLAIR mismatch estimation and identification of patients presenting within 4.5h from symptom onset.

Materials and methods: In this retrospective study, all pre-treatment and early follow-up (<48h post symptom onset) MRI datasets including DWI (b=0-1000 sec/mm^2) and FLAIR sequences obtained in consecutive patients with AIS referred for reperfusion therapies between January 2002 and May 2019 were included. On the training set (80%), a generative adversarial network was trained to produce synthetic FLAIR, using DWI as input. On the test set (20%), synthetic FLAIR was computed without real FLAIR knowledge. DWI-FLAIR mismatch was evaluated on both FLAIR by four independent readers. Inter-observer reproducibility and DWI-FLAIR mismatch concordance between synthetic and real FLAIR were evaluated with kappa statistics. Sensitivity and specificity for identification of AIS ≤4.5h were compared in patients with known onset time using McNemar test.

Results: 1416 MRI scans (861 patients, median [IQR] age: 71yrs [57-81]; 375 men) were included, yielding 1134 and 282 scans for training and test sets, respectively. Regarding DWI-FLAIR mismatch, inter-observer reproducibility was substantial for real and synthetic FLAIR (κ=0.80 [95%CI: 0.74-0.87] and 0.80 [0.74-0.87], respectively). After consensus, concordance between real and synthetic FLAIR was almost perfect (κ=0.88 [0.82-0.93]). Diagnostic value for identifying AIS ≤4.5h did not differ between real and synthetic FLAIR (sensitivity: 107/131 [82%] vs. 111/131 [85%], *P*=0.2; specificity: 96/104 [92%] vs. 96/104 [92%], *P*>.99, respectively).

Conclusion: Synthetic FLAIR had similar diagnostic performances to real FLAIR for DWI-FLAIR mismatch detection and identification of early acute ischemic stroke and may accelerate MRI protocols.

Introduction

Time of symptom onset is unknown in up to 27% of patients with acute ischemic stroke (AIS) (1), especially in the setting of wake-up stroke. Yet, knowledge of estimated time elapsed since stroke onset is part of current recommendations for reperfusion therapies (2). MRI plays an important role in estimating time since stroke onset: the presence of an acute ischemic lesion on diffusion-weighted imaging (DWI) in the absence of a hyperintense lesion on fluid-attenuated inversion recovery (FLAIR), DWI-FLAIR mismatch, indicates a short (≤4.5h) onset-to-MRI delay (3–5). The WAKE-UP stroke trial showed that in patients with AIS, unknown time of symptom onset and DWI-FLAIR mismatch, intravenous thrombolysis resulted in a better functional outcome than placebo (6). DWI-FLAIR mismatch may also help in selecting patients with unknown time of AIS onset for mechanical thrombectomy (7). FLAIR is also used to rule out subacute AIS (8) and stroke mimics, and for evaluating the extent of white matter hyperintensities (WMHs) (9). A FLAIR sequence is therefore part of most stroke MR protocols (10), regardless of whether AIS onset time is known.

Because time is of the essence in the management of AIS, short imaging baseline protocols are needed to allow for prompt treatment decisions (11). FLAIR sequence acquisition as part of an AIS MR protocol usually requires several minutes, and image quality may be suboptimal in restless patients (12). To overcome these limitations, attempts have been made to use the T2-weighted echo-planar imaging (EPI) sequence before the application of diffusion gradients (b=0 sec/mm^2 [b0]) as substitute for FLAIR (13). The resulting b0-DWI mismatch allowed estimation of AIS onset with a moderate sensitivity (72.9%), in part because analysis of cortical regions was hindered by high signal intensity from cerebrospinal fluid on the b0 images.

Based on the assumption that key T2-signal changes were embedded in the b0 and b=1000 s/mm^2 (b1000) weightings, we hypothesized that synthetic FLAIR images generated solely based on DWI using deep learning methods could compete with real FLAIR images for DWI-FLAIR mismatch determination. Such an approach may allow to omit FLAIR acquisition and thus reduce scan time in the acute stroke setting.

The purpose of our study was therefore to compare deep learning-derived synthetic FLAIR to real FLAIR images for presence of DWI-FLAIR mismatch and identification of patients with AIS imaged ≤4.5h of stroke onset.

Material and Methods

In accordance with French legislation, a commitment to compliance was filed under the reference MR4708101219. Patients were informed and offered the possibility to be excluded from data analysis. As this study implied retrospective analysis of anonymized data collected as part of routine care, approval by an Ethics Committee was not required and written informed consent was not requested as per MR-004 national regulation. Various parts of the population studied here have been published in 25 original manuscripts; however, synthetic FLAIR was not evaluated in any of these studies (Online Appendix). Data generated or analyzed during the study are available from the corresponding author by request.

Patients

We retrospectively included consecutive AIS patients admitted to our hospital between January 2002 and May 2019. The patients were identified from a prospectively collected stroke registry of consecutive patients. Patient were included in this study if they had

undergone acute stroke MRI before treatment and received reperfusion treatment, regardless of whether stroke onset time was known or not. Patients who refused to participate to the study were excluded. In this center, MRI has been used as a first-line diagnostic tool for acute AIS during this period (14). All baseline and early MRI follow-up examinations performed within 48 hours of hospital admission were included in the analysis and are thereafter termed MRI datasets. MRI datasets with missing DWI or FLAIR images were excluded. Age, sex, National Institutes of Health Stroke Scale score at admission, stroke onset-to-MRI delay, and recanalization treatment were collected.

MRI acquisition and parameters

MRI scans were acquired with a 1.5-T MRI scanner (Signa EchoSpeed; GE Healthcare) with a 33 mT/m gradient and an eight-channel coil, with similar parameters during the entire study period. DWI parameters were 128×128 matrix, 24-cm field of view, 6-mm slice thickness, repetition time 6400-6700 msec, echo time 90 msec, diffusion weightings: b=0 and b=1000 sec/mm^2, gradients applied in three orthogonal directions. ADC maps were computed based on DWI acquisition. FLAIR parameters were 256×192 matrix, 24-cm field-of-view, TR 8000-10000 msec, inversion time 2000-2300 msec. Sequence duration was 53 seconds for DWI and between 1 minute and 40 seconds (after 2018) and 2 minutes and 15 seconds (before 2018) for FLAIR (termed real FLAIR). Total protocol duration including time of flight angiography and T2-gradient-echo imaging was < 7 minutes.

Data preprocessing

Sequences were exported from the Picture Archiving and Communication System (PACS) and upscaled to a 256×256 matrix. Real FLAIR images were coregistered onto the corresponding DWI sequences using FSL FLIRT (version 6.0, Functional Magnetic Resonance Imaging of the Brain, Oxford, UK, non-commercial software) (15) with 12-parameters affine registration. The dataset was split into training and test sets (80/20%), with stratification regarding MRI time-point (baseline or early follow-up). MRI quality was evaluated by an independent reader (MAD, MSc, 3-months training in stroke imaging) on an ordinal scale ranging from 1 (low quality) to 3 (high quality).

Deep-learning model

The deep-learning model was derived from Ea-GAN (16) (see **Supplemental Material**). The model was trained on the training set using source DWI, ADC, and real FLAIR. After training was complete, synthetic FLAIR images were generated in the test set using source DWI and ADC maps but not real FLAIR images. Information for model architecture and training as well as an illustration of the network are provided in **Supplemental Material** and **Supplemental Figure 1**. Source code and model weights will be made freely available at https://github.com/NeuroSainteAnne/synthFLAIR. Total time for synthetic FLAIR calculation in the test set was measured on a production environment, and MR time reduction estimated in **Supplemental Figure 2**.

Data analysis in the test set

DWI (b1000) and ADC maps were displayed beside real FLAIR or synthetic FLAIR images, presented in random order. Four neuroradiologists (GH, JB, LL, CO with 3, 5, 10, 20 years of experience in stroke imaging, respectively), trained to the Wake-Up Radiology Trainer set (17) and blinded to FLAIR sequence type and onset-to-MRI delay, compared DWI and FLAIR images and determined whether an ischemic lesion was visible on FLAIR images. Each reader evaluated both synthetic FLAIR and real FLAIR images of assigned MRI datasets in separate sessions, with a two-month wash-out period between sessions to avoid recall bias. FLAIR lesion visibility was categorized as “Negative FLAIR” (i.e., presence of DWI-FLAIR mismatch), “Positive FLAIR” (i.e., absence of DWI-FLAIR mismatch), or “Non assessable”, as per Wake-Up Stroke trial specifications (18). The test dataset was split into 4 subsets. Each of the four readers were assigned 2 of these 4 subsets (**Supplemental Figure 3**); as a result, each MRI set was evaluated by two readers for inter-observer reproducibility assessment. Two months later, 2 readers each re-evaluated 1 data subset for intra-observer reproducibility assessment. Between-reader discrepancies were resolved by consensus. The visual analysis was complemented by a quantitative analysis of FLAIR signal changes. The relative signal intensity (rSI) of the ischemic lesion to the mirror lesion’s signal intensity in the contralateral hemisphere was calculated on real and synthetic FLAIR data (Supplemental Material) as described previously (5). Finally, a single neuroradiologist (JB) evaluated WMHs according to the modified Fazekas scale (19) on real FLAIR and synthetic FLAIR images, for the whole test set.

Statistical analysis

Statistical analysis was conducted with R (version 4.0.1, R Foundation, Vienna, Austria, open-source). Values are expressed as median (Interquartile range) and/or 95% CIs. Intra-observer reproducibility, inter-observer reproducibility, and concordance between real FLAIR and synthetic FLAIR for DWI-FLAIR mismatch were evaluated with Cohen Kappa coefficient. Sensitivity, specificity, positive predictive value, and negative predictive value of DWI-FLAIR mismatch for the identification of AIS≤4.5h were compared between real FLAIR and synthetic FLAIR using McNemar test, and relative predictive values method using DTComPair module (20). Pre-specified subgroup analyses were conducted on low-quality (score≤2) real FLAIR, and in patients imaged within 12h to focus the analysis on early MRI scans. Adjudication times and rSI were compared with Wilcoxon paired test. Concordance between real FLAIR and synthetic FLAIR for Fazekas scores was evaluated with weighted κ. Correlation coefficient of rSI measured on real and synthetic FLAIR was calculated using Pearson coefficient. Area under the ROC curve for the identification of AIS≤4.5h using rSI were computed and compared using DeLong's method. Statistical threshold for significance was $P = .05$.

Results

Patients

During the screening period, 1416 MRI datasets from 821 patients (446 women, 375 men, median age: 71y [IQR, 57-81]) were available (**Figure 1**), of which 1134 (80%) were used for

training and 282 (20%) for evaluation (test set). Clinical data are summarized in **Table 1**. In the test set, a lesion was seen on DWI in 280 of 282 (99%) MRI datasets.

Synthetic FLAIR generation and adjudication time

Median duration for synthetic FLAIR image generation was 2.5 seconds (IQR, 1.7-3.4). Median total duration for 24-slice DWI transfer onto the server, data conversion, synthetic FLAIR generation and transmission to PACS was 22.3 seconds (IQR, 17.9-25.0). Adjudication time for DWI-FLAIR mismatch assessment was similar between real FLAIR and synthetic FLAIR (median time: 13 seconds [IQR, 7-24] and 13 seconds [IQR, 8-26], respectively*; P*=.55).

Intra- and inter-observer reproducibility for FLAIR lesion visibility

Intra-observer reproducibility was almost perfect both for real FLAIR (κ=0.85 [95%CI: 0.76-0.93], range 0.84-0.86 per reader) and synthetic FLAIR (κ=0.85 [95%CI: 0.76-0.93], range 0.83-0.86 per reader). Inter-observer reproducibility was substantial (κ=0.80 [0.74-0.87] and κ=0.80 [95%CI: 0.74-0.87], respectively).

Concordance between real FLAIR and synthetic FLAIR

Intra-observer concordance is summarized for each reader in **Table 2**. After consensus, DWI-FLAIR mismatch was present in 133/282 (47%) and 138/282 (49%) MRI datasets with real FLAIR and synthetic FLAIR (**Supplemental Table 1**), respectively, and concordance between real FLAIR and synthetic FLAIR was almost perfect (κ=0.88 [95%CI: 0.82-0.93]). Illustrative examples are shown in **Figure 2**.

Identification of AIS with a time since onset ≤4.5hr with visual analysis

True stroke onset-to-MRI delay was available in 239 of 282 test MRI datasets (84%). Of these, 4 pairs were excluded due to non-assessable FLAIR (2 MRI datasets with non-assessable real FLAIR and 2 MRI datasets with non-assessable real FLAIR and synthetic FLAIR). Of the remaining 235 assessable MRI datasets, 131 were acquired within 4.5h after onset. There was no significant difference in sensitivity or specificity of DWI-FLAIR mismatch for identification of AIS≤4.5h using real FLAIR or synthetic FLAIR (107/131 [82%] vs. 111/131 [85%], *P*=.2; and 96/104 [92%] vs. 96/104 [92%], *P*>.99, respectively) (**Table 3**).

There was again no difference in sensitivity or specificity in the subgroup imaged within 12h of onset (n=145; 131/145 [90%] imaged ≤4.5h): 107/131 [82%] vs 111/131 [85%], *P*=.2; and 9/14 [64%] vs 10/14 [71%], *P*=.3, respectively.

Identification of AIS with a time since onset ≤4.5hr with quantitative analysis

In 239 MRI datasets with known onset-to-MRI delay, median rSI was 1.15 (IQR, 1.07-1.33) and 1.13 (IQR, 1.06-1.28) for real FLAIR and synthetic FLAIR, respectively (*P*=0.15). rSI values measured on real FLAIR and synthetic FLAIR were positively correlated (*r*=0.75 [95%CI: 0.69-0.80]). Area under the ROC curve for identification of AIS with a time since onset ≤4.5hr were not significantly different between real and synth FLAIR (0.87 [95%CI: 0.82-0.91] vs. 0.88 [95%CI: 0.83-0.92] respectively, *P*=.80) (**Figure 3**).

WMHs

Concordance for WMH scoring between real FLAIR and synthetic FLAIR was substantial (weighted-κ=0.76 [95%CI: 0.70-0.81]).

Discussion

Benefits of recanalization are highly time-dependent in AIS (11,21,22), thus minimizing the time for each step of the imaging workflow before treatment is crucial (23,24). We showed that synthetic FLAIR, generated solely from DWI, was highly consistent with real FLAIR for the evaluation of DWI-FLAIR mismatch, with results as accurate as real FLAIR for identifying AIS<4.5h after onset. This suggests that synthetic FLAIR may replace real FLAIR for that purpose in AIS.

MRI-based selection for AIS patients can be accomplished within a timeframe similar to CT-based selection without delaying treatment (23) and is associated with more favorable functional outcome and less mortality after mechanical thrombectomy (24). However, MRI scan duration is currently longer than CT and efforts are needed to shorten MR duration (23,24). To do so, multiple approaches have been proposed: using EPI-based sequences for T2 gradient-echo and FLAIR (12,25), applying multiband imaging (26), or quantitative MR imaging methods such as synthetic MRI (27). The latter approach produces parametric maps from which various MR contrasts, including FLAIR, can be calculated. However, synthetic MRI does not currently provide FLAIR images free of hyperintense artifacts (28), and EPI-based FLAIR cannot replace real FLAIR for stroke-to-MRI delay estimation because of lower accuracy for detecting signal changes (12). Rather than aiming at shortening FLAIR acquisition, our approach would allow to effectively omit it. We confirmed that FLAIR signal

changes in AIS are embedded in the b0 and b1000 weightings of the DWI sequence (13), allowing generation of synthetic FLAIR images that contain key information for identification of AIS with a time since onset ≤4.5hr, either visually using the DWI-FLAIR mismatch or quantitatively using the rSI. Moreover, synthetic FLAIR mimicked real FLAIR images, with equal labelling time, suggesting the absence of a learning curve.

Synthetic FLAIR has several advantages. First, it allows a ≈25% reduction in scanning time if real FLAIR acquisition is removed from MR protocol, with synthetic FLAIR being computed during the acquisition of the remaining sequences. Although it does not obviate the need to optimize each step of the workflow to minimize door-to-needle time, saving 1.66 min could theoretically avoid the loss of up to 3.1 million neurons (11). Second, synthetic FLAIR should allow motion artifact reduction in restless patients with approximately 10% not assessable FLAIR images based on previous studies (29). Each DWI image is acquired in <1 second, thus theoretically “freezing” head movements and minimizing severe artifacts. Synthetic FLAIR may also avoid repeated FLAIR acquisitions when there are severe motion artifacts in restless patients. Third, synthetic FLAIR is available once DWI is acquired, which is crucial whenever the MR is prematurely interrupted in restless patients with unknown stroke onset time. Fourth, synthetic FLAIR is directly comparable with DWI images, without the need for coregistration. Lastly, it allows an accurate evaluation of WMHs, which are considered a risk factor for post-thrombolysis hemorrhage (30) and for post- mechanical thrombectomy unfavorable outcome (9).

Our study has limitations. First, synthetic FLAIR was developed and tested on MRI scans from a single scanner with minimal variations in imaging parameters, and our findings cannot be directly inferred to other MR scanners. In any deep-learning application to medical imaging, using a single source of information increases between-subject

homogeneity and facilitates the learning process, even though it reduces generalizability. For further validation and to satisfy the Checklist for Artificial Intelligence in Medical Imaging, the algorithm needs validation on external data (31) with paired DWI and FLAIR image sets, ideally from different MR units and manufacturers. To this end, fine-tuning the freely-available learned model onto any new MR unit will likely be necessary (32). Unsupervised domain adaptation techniques may be an alternative approach allowing to implement our model onto a new image domain without the need for paired sets (33). Second, patients imaged in the intermediate known onset time window (i.e., 4.5-12h) were under-represented (namely, 10% of all patients imaged within 12h), as in previous studies (29,34). Indeed, with respect to our retrospective study, prehospital ultrafast workflow with immediate round-the-clock access to MR was dedicated to AIS patients eligible for reperfusion therapy, namely ≤3h until 2008, and subsequently ≤4.5h for intravenous thrombolysis and ≤6h for mechanical thrombectomy. To overcome this limitation, we chose to analyze MR datasets obtained before and early (≈24h) after recanalization treatment. Including MRI datasets with a wide range of onset-to-MRI delays was deemed necessary for the model to learn both on negative and positive FLAIR and avoid class imbalance. This naturally entails a higher sensitivity and specificity for identifying AIS with a time since onset ≤4.5hr as compared to previous studies (34), but does not prevent comparing the two types of FLAIR images. Finally, we cannot exclude that synthetic FLAIR may be less accurate for the detection of stroke mimics (35), since we only included AIS. Given that in this study T2 signal changes unrelated to the index stroke, such as WMHs, were equally well detected by both FLAIR image subtypes, synthetic FLAIR might also help to detect T2 signal changes in stroke mimics. However, synthetic FLAIR is unlikely to be as sensitive as real FLAIR for the detection

of acute subarachnoid hemorrhage, so real FLAIR or CT remain necessary whenever subarachnoid hemorrhage is suspected.

In conclusion, synthetic FLAIR may eventually replace real FLAIR sequences in the setting of AIS, allowing a clinically relevant shortening of stroke MR protocols while allowing similar diagnostic performance for DWI-FLAIR mismatch assessment. Prospective multicenter validation is needed to confirm the present findings.

References

1. Fink JN, Kumar S, Horkan C, Linfante I, Selim MH, Caplan LR, Schlaug G. The Stroke Patient Who Woke Up. Stroke 2002;33(4):988–993. doi: 10.1161/01.STR.0000014585.17714.67.

2. Powers WJ, Rabinstein AA, Ackerson T, Adeoye OM, Bambakidis NC, Becker K, Biller J, Brown M, Demaerschalk BM, Hoh B, Jauch EC, Kidwell CS, Leslie-Mazwi TM, Ovbiagele B, Scott PA, Sheth KN, Southerland AM, Summers DV, Tirschwell DL. Guidelines for the Early Management of Patients With Acute Ischemic Stroke: 2019 Update to the 2018 Guidelines for the Early Management of Acute Ischemic Stroke: A Guideline for Healthcare Professionals From the American Heart Association/American Stroke Association. Stroke 2019;50(12):e344–e418. doi: 10.1161/STR.0000000000000211.

3. Thomalla G, Cheng B, Ebinger M, Hao Q, Tourdias T, Wu O, Kim JS, Breuer L, Singer OC, Warach S, Christensen S, Treszl A, Forkert ND, Galinovic I, Rosenkranz M, Engelhorn T, Köhrmann M, Endres M, Kang D-W, Dousset V, Sorensen AG, Liebeskind DS, Fiebach JB, Fiehler J, Gerloff C, STIR and VISTA Imaging Investigators. DWI-FLAIR mismatch for the identification of patients with acute ischaemic stroke within 4·5 h of symptom onset (PRE-FLAIR): a multicentre observational study. Lancet Neurol 2011;10(11):978–986. doi: 10.1016/S1474-4422(11)70192-2.

4. Aoki J, Kimura K, Iguchi Y, Shibazaki K, Sakai K, Iwanaga T. FLAIR can estimate the onset time in acute ischemic stroke patients. J Neurol Sci 2010;293(1–2):39–44. doi: 10.1016/j.jns.2010.03.011.

5. Petkova M, Rodrigo S, Lamy C, Oppenheim G, Touzé E, Mas J-L, Méder J-F, Oppenheim C. MR imaging helps predict time from symptom onset in patients with acute

stroke: implications for patients with unknown onset time. Radiology 2010;257(3):782–792.

6. Thomalla G, Simonsen CZ, Boutitie F, Andersen G, Berthezene Y, Cheng B, Cheripelli B, Cho T-H, Fazekas F, Fiehler J, Ford I, Galinovic I, Gellissen S, Golsari A, Gregori J, Günther M, Guibernau J, Häusler KG, Hennerici M, Kemmling A, Marstrand J, Modrau B, Neeb L, Perez de la Ossa N, Puig J, Ringleb P, Roy P, Scheel E, Schonewille W, Serena J, Sunaert S, Villringer K, Wouters A, Thijs V, Ebinger M, Endres M, Fiebach JB, Lemmens R, Muir KW, Nighoghossian N, Pedraza S, Gerloff C. MRI-Guided Thrombolysis for Stroke with Unknown Time of Onset. N Engl J Med 2018;379(7):611–622. doi: 10.1056/NEJMoa1804355.

7. Escalard S, Gory B, Kyheng M, Desilles J-P, Redjem H, Ciccio G, Smajda S, Labreuche J, Mazighi M, Piotin M, Blanc R, Lapergue B, Fahed R, of the ETIS (Endovascular Treatment in Ischemic Stroke) Research Investigators. Unknown-onset strokes with anterior circulation occlusion treated by thrombectomy after DWI-FLAIR mismatch selection. Eur J Neurol 2018;25(5):732–738. doi: 10.1111/ene.13580.

8. Tisserand M, Le Guennec L, Touzé E, Hess A, Charbonnier C, Devauchelle A-D, Bracard S, Mas J-L, Méder J-F, Oppenheim C. Prevalence of MRI-defined recent silent ischemia and associated bleeding risk with thrombolysis. Neurology 2011;76(15):1288–1295. doi: 10.1212/WNL.0b013e3182152855.

9. Boulouis G, Bricout N, Ben Hassen W, Ferrigno M, Turc G, Bretzner M, Benzakoun J, Seners P, Personnic T, Legrand L, Trystram D, Rodriguez-Regent C, Charidimou A, Rost NS, Bracard S, Cordonnier C, Oppenheim C, Naggara O, Henon H. White matter hyperintensity burden in patients with ischemic stroke treated with thrombectomy. Neurology 2019;93(16):e1498–e1506. doi: 10.1212/WNL.0000000000008317.

10. Leiva-Salinas C, Wintermark M. Imaging of Ischemic Stroke. Neuroimaging Clin N Am. 2010;20(4):455–468. doi: 10.1016/j.nic.2010.07.002.

11. Saver JL. Time is brain--quantified. Stroke 2006;37(1):263–266. doi: 10.1161/01.STR.0000196957.55928.ab.

12. Benzakoun J, Maïer B, Calvet D, Edjali M, Turc G, Lion S, Legrand L, Ben Hassen W, Naggara O, Meder JF, Mas JL, Oppenheim C. Can a 15-sec FLAIR replace conventional FLAIR sequence in stroke MR protocols? J Neuroradiol 2017;44(3):192–197. doi: 10.1016/j.neurad.2016.11.001.

13. Geraldo AF, Berner L-P, Haesebaert J, Chabrol A, Cho T-H, Derex L, Hermier M, Louis-Tisserand G, Chamard L, Klaerke Mikkelsen I, Ribe L, Østergaard L, Hjort N, Pedraza S, Thomalla G, Baron J-C, Nighoghossian N, Berthèzene Y. Does b1000–b0 Mismatch Challenge Diffusion-Weighted Imaging–Fluid Attenuated Inversion Recovery Mismatch in Stroke? Stroke 2016;STROKEAHA.115.011501. doi: 10.1161/STROKEAHA.115.011501.

14. Accident vasculaire cérébral : prise en charge précoce (alerte, phase préhospitalière, phase hospitalière initiale, indications de la thrombolyse). Haute Aut. Santé. https://www.has-sante.fr/jcms/c_830203/fr/accident-vasculaire-cerebral-prise-en-charge-precoce-alerte-phase-prehospitaliere-phase-hospitaliere-initiale-indications-de-la-thrombolyse. Published June 23, 2010. Accessed May 22, 2020.

15. Jenkinson M, Smith S. A global optimisation method for robust affine registration of brain images. Med Image Anal. 2001;5(2):143–156. doi: 10.1016/s1361-8415(01)00036-6.

16. Yu B, Zhou L, Wang L, Shi Y, Fripp J, Bourgeat P. Ea-GANs: Edge-Aware Generative Adversarial Networks for Cross-Modality MR Image Synthesis. IEEE Trans Med Imaging. 2019;38(7):1750–1762. doi: 10.1109/TMI.2019.2895894.

17. Galinovic I, Puig J, Neeb L, Guibernau J, Kemmling A, Siemonsen S, Pedraza S, Cheng B, Thomalla G, Fiehler J, Fiebach JB. Visual and region of interest-based inter-rater agreement in the assessment of the diffusion-weighted imaging- fluid-attenuated inversion

recovery mismatch. Stroke 2014;45(4):1170–1172. doi: 10.1161/STROKEAHA.113.002661.

18. Thomalla G, Fiebach JB, Østergaard L, Pedraza S, Thijs V, Nighoghossian N, Roy P, Muir KW, Ebinger M, Cheng B, Galinovic I, Cho T-H, Puig J, Boutitie F, Simonsen CZ, Endres M, Fiehler J, Gerloff C, WAKE-UP investigators. A multicenter, randomized, double-blind, placebo-controlled trial to test efficacy and safety of magnetic resonance imaging-based thrombolysis in wake-up stroke (WAKE-UP). Int J Stroke 2014;9(6):829–836. doi: 10.1111/ijs.12011.

19. Pantoni L, Basile AM, Pracucci G, Asplund K, Bogousslavsky J, Chabriat H, Erkinjuntti T, Fazekas F, Ferro JM, Hennerici M, O'brien J, Scheltens P, Visser MC, Wahlund L-O, Waldemar G, Wallin A, Inzitari D. Impact of age-related cerebral white matter changes on the transition to disability - the LADIS study: rationale, design and methodology. Neuroepidemiology. 2005;24(1–2):51–62. doi: 10.1159/000081050.

20. Stock C, Hielscher T. DTComPair: Comparison of binary diagnostic tests in a paired study design. https://cran.r-project.org/web/packages/DTComPair/index.html. Published February 16, 2014. Accessed January 7, 2016.

21. Goyal M, Demchuk AM, Menon BK, Eesa M, Rempel JL, Thornton J, Roy D, Jovin TG, Willinsky RA, Sapkota BL, Dowlatshahi D, Frei DF, Kamal NR, Montanera WJ, Poppe AY, Ryckborst KJ, Silver FL, Shuaib A, Tampieri D, Williams D, Bang OY, Baxter BW, Burns PA, Choe H, Heo J-H, Holmstedt CA, Jankowitz B, Kelly M, Linares G, Mandzia JL, Shankar J, Sohn S-I, Swartz RH, Barber PA, Coutts SB, Smith EE, Morrish WF, Weill A, Subramaniam S, Mitha AP, Wong JH, Lowerison MW, Sajobi TT, Hill MD. Randomized Assessment of Rapid Endovascular Treatment of Ischemic Stroke. N Engl J Med 2015;372(11):1019–1030. doi: 10.1056/NEJMoa1414905.

22. Menon BK, Sajobi TT, Zhang Y, Rempel JL, Shuaib A, Thornton J, Williams D, Roy D,

Poppe AY, Jovin TG, Sapkota B, Baxter BW, Krings T, Silver FL, Frei DF, Fanale C, Tampieri D, Teitelbaum J, Lum C, Dowlatshahi D, Eesa M, Lowerison MW, Kamal NR, Demchuk AM, Hill MD, Goyal M. Analysis of Workflow and Time to Treatment on Thrombectomy Outcome in the Endovascular Treatment for Small Core and Proximal Occlusion Ischemic Stroke (ESCAPE) Randomized, Controlled Trial. Circulation 2016;133(23):2279–2286. doi: 10.1161/CIRCULATIONAHA.115.019983.

23. Provost C, Soudant M, Legrand L, Ben Hassen W, Xie Y, Soize S, Bourcier R, Benzakoun J, Edjlali M, Boulouis G, Raoult H, Guillemin F, Naggara O, Bracard S, Oppenheim C. Magnetic Resonance Imaging or Computed Tomography Before Treatment in Acute Ischemic Stroke. Stroke 2019;50(3):659–664. doi: 10.1161/STROKEAHA.118.023882.

24. Meinel TR, Kaesmacher J, Mosimann PJ, Seiffge D, Jung S, Mordasini P, Arnold M, Goeldlin M, Hajdu SD, Olivé-Gadea M, Maegerlein C, Costalat V, Pierot L, Schaafsma JD, Fischer U, Gralla J. Association of initial imaging modality and futile recanalization after thrombectomy. Neurology 2020;95(17):e2331–e2342. doi: 10.1212/WNL.0000000000010614.

25. Nael K, Khan R, Choudhary G, Meshksar A, Villablanca P, Tay J, Drake K, Coull BM, Kidwell CS. Six-Minute Magnetic Resonance Imaging protocol for evaluation of acute ischemic stroke: pushing the boundaries. Stroke 2014;45(7):1985–1991. doi: 10.1161/STROKEAHA.114.005305.

26. Skare S, Sprenger T, Norbeck O, Rydén H, Blomberg L, Avventi E, Engström M. A 1-minute full brain MR exam using a multicontrast EPI sequence. Magn Reson Med 2018;79(6):3045–3054. doi: https://doi.org/10.1002/mrm.26974.

27. Tanenbaum LN, Tsiouris AJ, Johnson AN, Naidich TP, DeLano MC, Melhem ER, Quarterman P, Parameswaran SX, Shankaranarayanan A, Goyen M, Field AS. Synthetic MRI

for Clinical Neuroimaging: Results of the Magnetic Resonance Image Compilation (MAGiC) Prospective, Multicenter, Multireader Trial. Am J Neuroradiol 2017;38(6):1103–1110. doi: 10.3174/ajnr.A5227.

28. Ryu KH, Baek HJ, Moon JI, Choi BH, Park SE, Ha JY, Jeon KN, Bae K, Choi DS, Cho SB, Lee Y, Heo YJ. Initial clinical experience of synthetic MRI as a routine neuroimaging protocol in daily practice: A single-center study. J Neuroradiol 2020;47(2):151–160. doi: 10.1016/j.neurad.2019.03.002.

29. Thomalla G, Rossbach P, Rosenkranz M, Siemonsen S, Krützelmann A, Fiehler J, Gerloff C. Negative fluid-attenuated inversion recovery imaging identifies acute ischemic stroke at 3 hours or less. Ann Neurol. 2009;65(6):724–732. doi: 10.1002/ana.21651.

30. Lin Q, Li Z, Wei R, Lei Q, Liu Y, Cai X. Increased risk of post-thrombolysis intracranial hemorrhage in acute ischemic stroke patients with leukoaraiosis: a meta-analysis. PloS One 2016;11(4):e0153486. doi: 10.1371/journal.pone.0153486.

31. Mongan J, Moy L, Kahn CE. Checklist for Artificial Intelligence in Medical Imaging (CLAIM): A Guide for Authors and Reviewers. Radiol Artif Intell 2020;2(2):e200029. doi: 10.1148/ryai.2020200029.

32. Tajbakhsh N, Shin JY, Gurudu SR, Hurst RT, Kendall CB, Gotway MB, Liang J. Convolutional Neural Networks for Medical Image Analysis: Full Training or Fine Tuning? IEEE Trans Med Imaging 2016;35(5):1299–1312. doi: 10.1109/TMI.2016.2535302.

33. Novosad P, Fonov V, Collins DL. Unsupervised domain adaptation for the automated segmentation of neuroanatomy in MRI: a deep learning approach. bioRxiv 2019;845537. doi: 10.1101/845537. Published November 16, 2019. Accessed May 25, 2021.

34. Emeriau S, Serre I, Toubas O, Pombourcq F, Oppenheim C, Pierot L. Can diffusion-weighted imaging-fluid-attenuated inversion recovery mismatch (positive diffusion-weighted

imaging/negative fluid-attenuated inversion recovery) at 3 Tesla identify patients with stroke at <4.5 hours? Stroke. 2013;44(6):1647–1651. doi: 10.1161/STROKEAHA.113.001001.

35. Danière F, Edjlali-Goujon M, Mellerio C, Turc G, Naggara O, Tselikas L, Ben Hassen W, Tisserand M, Lamy C, Souillard-Scemama R, Flais S, Meder JF, Oppenheim C. MR screening of candidates for thrombolysis: How to identify stroke mimics? J Neuroradiol 2014;41(5):283–295. doi: 10.1016/j.neurad.2014.05.008.

Supplemental material

rSI computation

All ischemic lesions were segmented by a single radiologist (JB), using a combination of ADC thresholding at 620×10^{-6} mm^2/s and manual correction of the three-dimensional regions of interest (ROI) using Mango software (version 4.0.1, Research Imaging Institute, San Antonio, Texas, non-commercial software). As synthetic FLAIR values are scalars expressed between -1 and +1, a normalization procedure was performed on each synthetic FLAIR to match the mean and standard deviation of signal intensity of the corresponding real FLAIR. This normalization was done by selecting in-brain voxels outside of the DWI lesion in order to prevent cross-contamination. All DWI were then registered to the MNI152 brain atlas (Montreal Neurologic Institute, Montreal, Canada) using FSL FLIRT (version 6.0, Functional Magnetic Resonance Imaging of the Brain, Oxford, UK) and the quality of the registration was visually checked. The ROI was projected onto the MNI152 brain atlas, flipped onto the contralesional hemisphere, and then back-projected onto the original MRI acquisition referential, using a nearest-neighbor interpolation. The ADC maps were used to exclude voxels containing cerebrospinal fluid by excluding voxels with ADC values $>1200\times10^{-6}$ mm^2/s in both ROIs. The rSI was then computed by dividing the mean signal value in lesional ROI by the mean signal value in mirror ROI in both the real and synthetic FLAIR images.

Brain segmentation and weighting

To focus the learning process on the ischemic lesion and not on the normal brain tissue, three regions with different learning weights were defined:

- Ischemic region with high (×100) weighting
- Normal brain region with normal (×1) weighting
- Areas outside the brain with low (×0.01) weighting

To define the ischemic region, a loose ROI was manually drawn onto b1000 sequence using Mango software (version 4.0.1, Research Imaging Institute, San Antonio, Texas, non-commercial software) by a single reader (MAD, who did not participate in final evaluation of model performances). This loose ROI was intersected with a binary mask of ADC map, thresholded to remove cerebrospinal fluid areas. To define normal brain region, the ischemic region was subtracted to a brain mask computed with Brain Extracting Tool from FSL toolbox (version 6.0, Functional Magnetic Resonance Imaging of the Brain, Oxford, UK, non-commercial software).

Conditional architecture

Several FLAIR images presented slight motion artifacts in phase orientation, which were reproduced by the GAN in preliminary tests. To remove these artifacts from reconstruction without excluding a large data subset, we chose a conditional architecture, that included these artifacts as additional input in our Generator. A single reader (MAD, who did not participate in final evaluation of model performances) classified real FLAIR quality for all MRI datasets on an ordinal scale between 1 (low quality: important movement artifacts), 2 (moderate quality: few artifacts that did not impair interpretation) and 3 (excellent quality). This scalar was termed as *quality* scalar.

Model architecture

The EA-GAN model was composed of a Generator and a Discriminator (**Supplemental Figure 1**).

Generator

The Generator aims at constructing synthetic FLAIR images based on four inputs:

- DWI with b=1000 s/mm^2 trace weighting
- b=0 s/mm^2 weighting corresponding to the EPI sequence without diffusion gradients
- ADC map
- FLAIR quality as a conditional scalar (in learning mode only and set to maximum quality for synthetic FLAIR generation in the test set).

The Generator had a U-Net architecture, with a series of downward convolutions and upward convolutions linked by skip connections. The detailed architecture was:

- Five downward convolution blocks, each consisting of:
  - One 3×3 2D convolution layer
  - One 3×3 2D convolution layer with 2×2 strides
  - One Batch Normalization Layer
  - An activation layer with ReLu function
  - An increasing filters number (64, 128, 256, 512 and 1024) for each block
- Five upward convolution blocks, each consisting of:
  - One 3x3 2D transpose convolution layer with 2x2 strides
  - Two 3x3 2D convolution layers
  - One Batch Normalization Layer
  - An activation layer with ReLu function

- A decreasing filters number (512, 256, 128, 64 and 64) for each block

- One output layer with Tanh activation function

The correspondence between real FLAIR and synthetic FLAIR is ensured by the $\mathcal{L}_1$ loss:

$$\mathcal{L}_1 = \|y - G(x)\|_1$$

where x is the generator input, y is the value of the real FLAIR image and $G(x)$ is the image produced by the generator (synthetic FLAIR).

The edge-aware GAN architecture has been proposed by Yu et al. (16). The principle consisted in adding a supplemental loss between edges of generated image and of target image in order to overweight the importance of edges definition in the learning process. This aimed at increasing fine-grain definition of the brain contours. The edges maps were computed with a Sobel filter in two dimensions, and the following loss was added to the training:

$$\mathcal{L}_{Edge} = \|S(y) - S(G(x,q))\|_1$$

where S is the Sobel filter.

Adjunction of this supplemental loss allowed to improve synthesis quality by increasing the definition of FLAIR edges in a preliminary study on 24 test subjects (which did not serve for the main analysis) as compared to the classic Pix2Pix architecture.

Discriminator

The Discriminator discriminated the synthetic FLAIR and real FLAIR into a binary decision: synthetic or real (1 or 0). It took into input the following quintuplet:

- DWI with b=1000 s/mm^2 trace weighting
- b=0 s/mm^2 weighting corresponding to the EPI sequence without diffusion gradients
- ADC map
- FLAIR sequence (real or synthetic)
- Edge map of the FLAIR sequence

The discriminator had a downward architecture, and its output ranged between 0 and 1:

- Four downward convolution blocks, each consisting of:
  - One 4×4 2D convolution layer with 2×2 strides
  - One Batch Normalization Layer
  - An activation layer with ReLu function
  - For each block, the number of filters was increasing (64, 128, 256 and 512)
- 1 output 2×2 convolution layer with 2×2 strides and sigmoid activation function

The optimal prediction of the Discriminator was ensured by maximizing a result of 0 when real FLAIR was given as input and 1 when synthetic FLAIR was given as input. Hence, the following Discriminator Loss was:

$$\mathcal{L}_D = \|\log D(x,y,S(y)) + \log(1 - D(x,G(x),S(G(x))\|_1$$

where x is the DWI input, y the real FLAIR input, S(y) the sobel filter applied to real FLAIR and D(x, y ,S(y)) the result of Discriminator prediction for real FLAIR evaluation.

Generator Loss

The net Generator Loss was constructed with the $\mathcal{L}_1$ and $\mathcal{L}_{Edge}$. An additional term was added such as the loss decreased when the Discriminator output reached 0 when synthetic FLAIR was given as its input. Hence, the following overall Generator Loss was:

$$\mathcal{L}_G = \left\|\lambda_1 \times \mathcal{L}_1 + \lambda_{Edge} \times \mathcal{L}_{Edge} + \log D(x,G(x),S(G(x))\right\|_1$$

where λ_1 and λ_{Edge} were two weighting constants for learning process.

Model training

The MRI dataset was split between a training and a test set with an 80/20% split. Within the training set, 80% of the MRIs were randomly selected for training purposes and 20% were kept aside for validation purposes (validation set). The model was trained on the training subset using Adam optimizer with a learning rate at 0.00001. Training was pursued during 3000 epochs. λ_1 value was set at 100. λ_{Edge} value increased from 1 to 100 during the first 100 epochs then was fixed at 100. Each 10 epochs, inference was made on the validation set and a visual map with several synthetic FLAIR and real FLAIR slices was saved. As the interpretation of model loss was not unambiguous, all visual maps were screened by a unique reader who selected the trained model with best visual features (2500^{th} model) for final inference on test model.

The models were developed on Tensorflow v2.0. All training sessions were done inside a JupyterLab notebook running on a python framework v3.7.3 in a Linux environment (Ubuntu 18.04 LTS). The training was done on a custom computer station with 2 TITAN RTX GPUs (with 2x24GB VRAM), on Intel i9-9900K CPU with 8 cores and 16 threads, 62 GB RAM and a 500-GB Solid State Drive.

Radiological evaluation

In order to evaluate each MRI set twice with four neuroradiologists, the test set was split into 4 subsets (A, B, C, and D). Each neuroradiologist evaluated stroke visibility on real FLAIR and synthetic FLAIR for two subsets: reader 1 evaluated subsets A and B, reader 2 evaluated subsets B and C, reader 3 evaluated subsets C and D and reader 4 evaluated subsets A and D. For intra-observer reproducibility, two months later, readers 1 and 2 reevaluated

respectively subsets A and B. The corresponding protocol is depicted in Supplemental Figure 2.

Tables

Table 1: Patient Characteristics in Training and Test Sets

Variable	Training Set	Test Set
No. of MRI datasets	1134	282
No. of MRI datasets with known onset-to-MRI delay	973 (86)	239 (84)
Onset-to-MRI delay (h)*	3.3 (1.8-25.6)	3.1 (1.9-24.0)
No. of patients	749	253
Age (y)*	70 (57-81)	71 (58-81)
No. of women	337 (45)	109 (43)
NIHSS score at admission*	14 (8-20)	15 (8-20)
Recanalization treatment		
- **IVT only**	474 (64)	163 (64)
- **MT only**	129 (17)	35 (14)
- **IVT + MT**	123 (16)	50 (20)
- **Missing data**	23 (3)	5 (2)

Note.— Data are expressed as number of patients, with percentages in parentheses. NIHSS = National Institutes of Health Stroke Scale, IVT = intravenous thrombolysis, MT = mechanical thrombectomy.

*Data are expressed as medians with interquartile range in parentheses.

Table 2: Intra-reader Concordance between Real FLAIR and Synthetic FLAIR Labeling

Variable	Reader 1	Reader 2	Reader 3	Reader 4	All Readers after Consensus
No. of MRI datasets	143	138	139	144	282
Concordance between real and synthetic FLAIR*	0.88 (0.80-0.96)	0.75 (0.65, 0.86)	0.73 (0.63, 0.83)	0.84 (0.76, 0.93)	0.88 (0.82, 0.93)

Note.— FLAIR = fluid-attenuated inversion recovery. *Data are expressed as κ values, with 95% CIs in parentheses.

Table 3: Comparison of DWI-FLAIR Mismatch Diagnostic Value using Real FLAIR and Synthetic FLAIR for the Identification of ≤4.5h Acute Ischemic Stroke

Statistic	Real FLAIR	Synthetic FLAIR	*P* Value
Sensitivity	107/131 (82%) [74, 87]	111/131 (85%) [78, 90]	0.2
Specificity	96/104 (92%) [86, 96]	96/104 (92%) [86, 96]	0.92
Positive predictive value	107/115 (93%) [87, 96]	111/119 (93%) [87, 97]	0.88
Negative predictive value	96/120 (80%) [72, 86]	96/116 (83%) [75, 89]	0.21

Note.— Diagnostic value was computed in the 235 MRI datasets where stroke onset-to-MRI delay was available and both real fluid-attenuated inversion recovery (FLAIR) and synthetic FLAIR images were assessable. Data are expressed as number of MRI datasets, with corresponding percentages in parentheses and 95% CIs in brackets. Sensitivities and specificities were compared using McNemar test; positive and negative predictive values were compared using relative predictive values.

Supplemental tables

Supplemental Table: Concordance between real FLAIR and synthetic FLAIR after consensus procedure

Variable	DWI-FLAIR mismatch with real FLAIR	No DWI-FLAIR mismatch with real FLAIR	Non-assessable with real FLAIR	Total
DWI-FLAIR mismatch with synthetic FLAIR	127	9	2	138
No DWI-FLAIR mismatch with synthetic FLAIR	6	133	1	140
Non-assessable with synthetic FLAIR	0	0	4	4
Total	133	142	7	282

Note.— Data are expressed as no. of MRI datasets. DWI = diffusion weighted imaging, FLAIR = fluid-attenuated inversion recovery

Figures legends

Figure 1: Flowchart for patient inclusion.

DWI = diffusion-weighted imaging, FLAIR = fluid-attenuated inversion recovery.

Figure 2: Comparison of DWI-FLAIR mismatch using real FLAIR and synthetic FLAIR in acute ischemic stroke.

DWI = diffusion-weighted imaging, FLAIR = fluid-attenuated inversion recovery.

A. DWI-FLAIR mismatch on synthetic FLAIR and real FLAIR in a 46-year-old woman with sudden right hemiplegia, aphasia, and dysarthria. On DWI obtained 2h after onset, hyperintensities are seen in the left middle cerebral artery without corresponding signal changes on real or synthetic FLAIR images.

B. No DWI-FLAIR mismatch on synthetic FLAIR and real FLAIR in 47-year-old man with sudden right hemiparesia. On DWI obtained 5h after onset, small hyperintensity is seen in the left internal capsula (arrowheads), also visible on real and synthetic FLAIR images.

C. No DWI-FLAIR mismatch on synthetic FLAIR and real FLAIR in 86-year-old woman with sudden right hemiplegia 5 h and 10 min before MRI. On DWI obtained 5h and 10 min after onset, large hyperintensity is seen in the left middle cerebral artery, also visible on real and synthetic FLAIR images. Of note, white matter hyperintensities (arrowheads) are equally seen on real and synthetic FLAIR images (Fazekas 2).

D. DWI-FLAIR mismatch on synthetic FLAIR and non-assessable real FLAIR in 47-year-old woman with sudden right hemiplegia and aphasia. On DWI obtained 2h after onset, hyperintensity is seen in the left middle cerebral artery territory. Real FLAIR was quoted as non-assessable because of severe motion artifact, whereas synthetic FLAIR is of diagnostic value, without signal intensity changes.

Figure 3: Performance of relative Signal Intensity (rSI) for identification of ≤4.5h ischemic stroke

In 239 MRI datasets with known onset-to-MRI delay, the area under the ROC curve was not significantly different between real FLAIR (0.87 [95%CI: 0.82-0.91]) and synthetic FLAIR (0.88 [95%CI: 0.83-0.92], P=.80). FLAIR = fluid-attenuated inversion recovery.

Supplemental figures

Supplemental Figure 1: EA-GAN architecture for generation of synthetic FLAIR sequences.

Convolutional neural network schematic was constructed with PlotNeuralNet tool (https://doi.org/10.5281/zenodo.2526396). ADC = apparent diffusion coefficient, b0 = diffusion gradient with b=0 sec/mm^2, b1000 = diffusion gradient with b=1000 sec/mm^2, DWI = diffusion-weighted imaging, FLAIR = fluid-attenuated inversion recovery, realFLAIR = real FLAIR, real Edges = edges map of real FLAIR, synthFLAIR = synthetic FLAIR, synth Edges = edges map of synthetic FLAIR, $\mathcal{L}_1$= L1 loss, $\mathcal{L}_{Edge}$= L1 loss applied to edges map, $\mathcal{L}_D$= discriminator loss.

Supplemental Figure 2: Acquisition time reduction.

Duration of the latest stroke MR protocol in our institution is depicted. By removing real FLAIR acquisition and computing the synthetic FLAIR sequence during 3D TOF MR angiogram acquisition, the total duration would benefit from a 26% reduction, notwithstanding PWI. Loc. = localizer sequences, DWI = diffusion-weighted imaging, FLAIR = fluid-attenuated inversion recovery, TOF = time-of-flight angiogram, PWI = perfusion-weighted imaging, sF = synthetic FLAIR computation.

Supplemental Figure 3: FLAIR evaluation process.

All patients in test set were evaluated by two distinct readers for interobserver reproducibility. Half of the test set was used for intraobserver reproducibility assessment.

Concordance between real FLAIR and synthetic FLAIR was assessed first for each reader then after consensus. Number of MRI datasets in each group is shown. FLAIR = fluid-attenuated inversion recovery, realFLAIR = real FLAIR, synthFLAIR = synthetic FLAIR

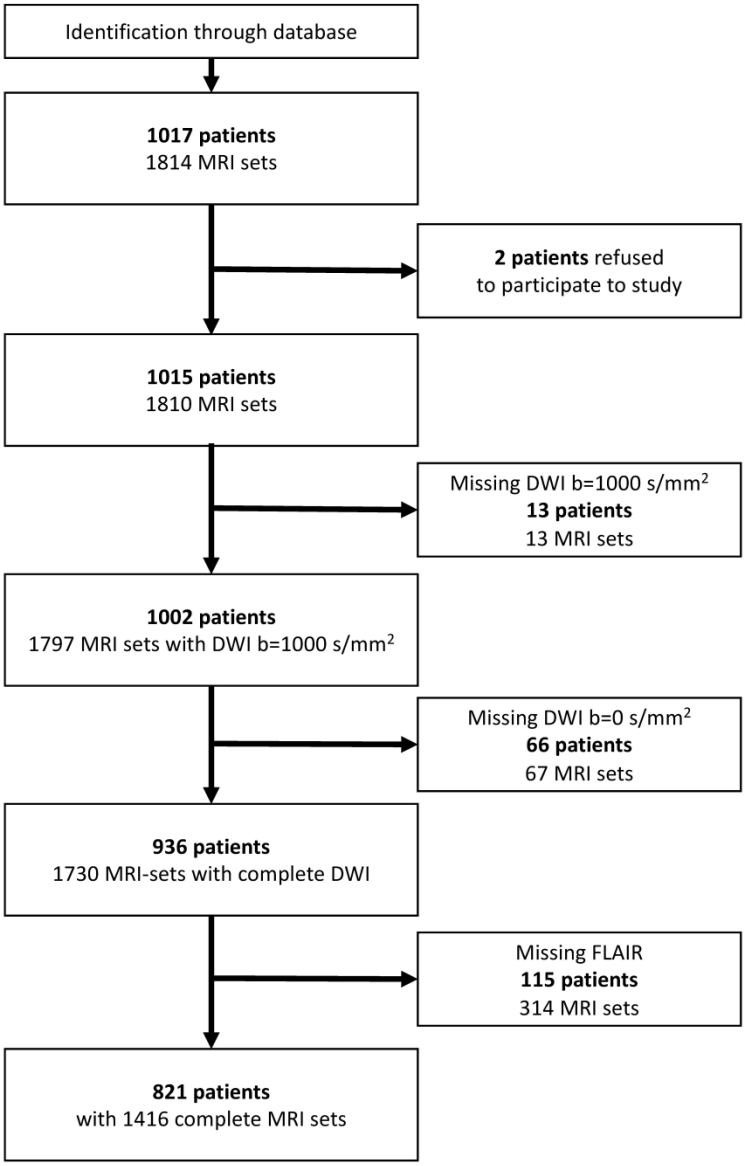

Figure 1: Flowchart for patient inclusion.
DWI = diffusion-weighted imaging, FLAIR = fluid-attenuated inversion recovery.

210x297mm (600 x 600 DPI)

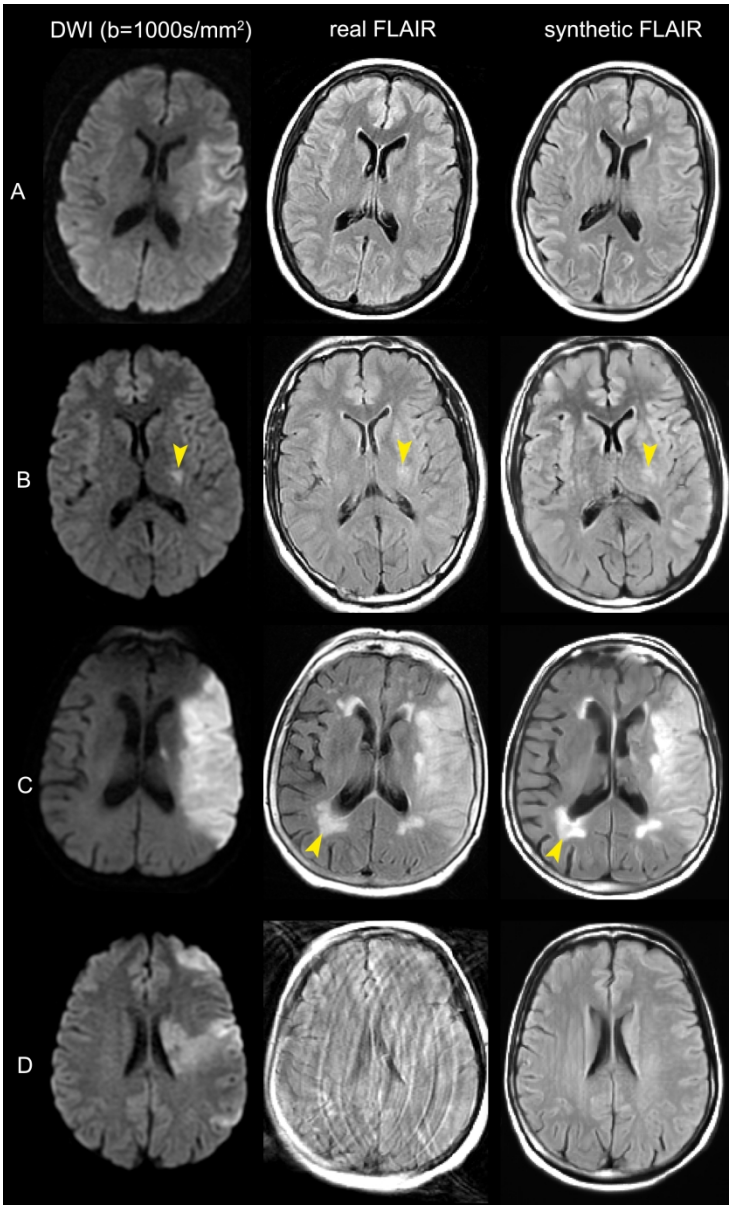

Figure 2: Comparison of DWI-FLAIR mismatch using real FLAIR and synthetic FLAIR in acute ischemic stroke.

DWI = diffusion-weighted imaging, FLAIR = fluid-attenuated inversion recovery.

A. DWI-FLAIR mismatch on synthetic FLAIR and real FLAIR in a 46-year-old woman with sudden right hemiplegia, aphasia, and dysarthria. On DWI obtained 2h after onset, hyperintensities are seen in the left middle cerebral artery without corresponding signal changes on real or synthetic FLAIR images.
B. No DWI-FLAIR mismatch on synthetic FLAIR and real FLAIR in 47-year-old man with sudden right hemiparesia. On DWI obtained 5h after onset, small hyperintensity is seen in the left internal capsula (arrowheads), also visible on real and synthetic FLAIR images.
C. No DWI-FLAIR mismatch on synthetic FLAIR and real FLAIR in 86-year-old woman with sudden right hemiplegia 5 h and 10 min before MRI. On DWI obtained 5h and 10 min after onset, large hyperintensity is seen in the left middle cerebral artery, also visible on real and synthetic FLAIR images. Of note, white

matter hyperintensities (arrowheads) are equally seen on real and synthetic FLAIR images (Fazekas 2). D. DWI-FLAIR mismatch on synthetic FLAIR and non-assessable real FLAIR in 47-year-old woman with sudden right hemiplegia and aphasia. On DWI obtained 2h after onset, hyperintensity is seen in the left middle cerebral artery territory. Real FLAIR was quoted as non-assessable because of severe motion artifact, whereas synthetic FLAIR is of diagnostic value, without signal intensity changes.

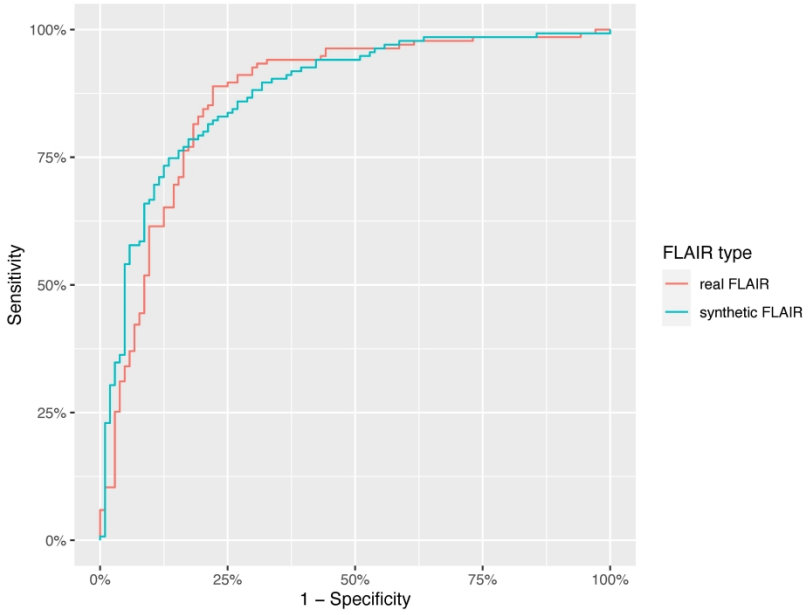

Caption : Figure 3: Performance of relative Signal Intensity (rSI) for identification of ≤4.5h ischemic stroke In 239 MRI sets with known onset-to-MRI delay, the area under the ROC curve was not significantly different between real FLAIR (0.87 [95%CI: 0.82-0.91]) and synthetic FLAIR (0.88 [95%CI: 0.83-0.92], P=.80). FLAIR = fluid-attenuated inversion recovery.

210x297mm (600 x 600 DPI)

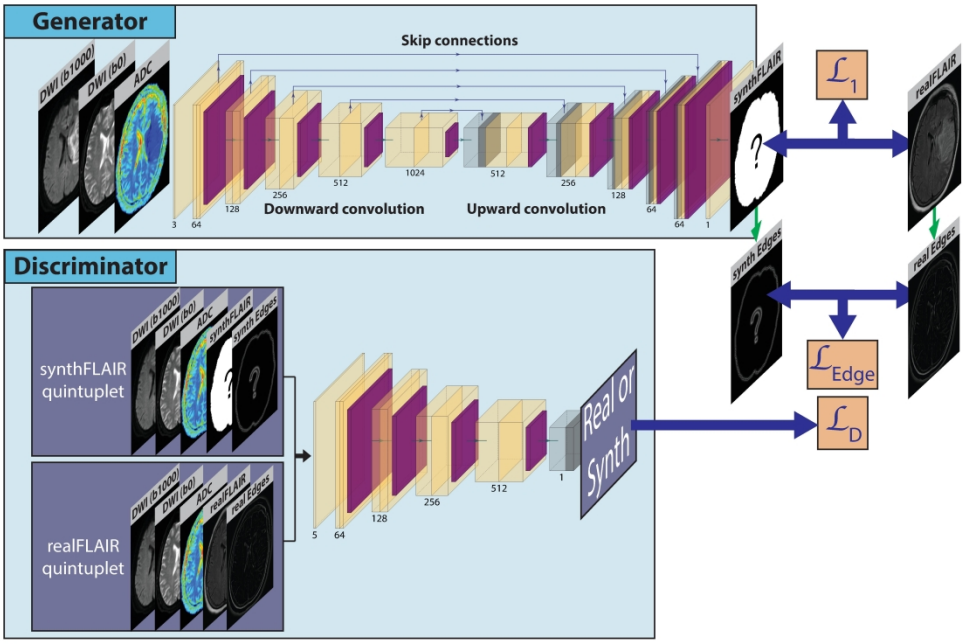

Supplemental Figure 1: EA-GAN architecture for generation of synthetic FLAIR sequences. Convolutional neural network schematic was constructed with PlotNeuralNet tool (https://doi.org/10.5281/zenodo.2526396). ADC = apparent diffusion coefficient, b0 = diffusion gradient with b=0 sec/mm2, b1000 = diffusion gradient with b=1000 sec/mm2, DWI = diffusion-weighted imaging, FLAIR = fluid-attenuated inversion recovery, realFLAIR = real FLAIR, real Edges = edges map of real FLAIR, synthFLAIR = synthetic FLAIR, synth Edges = edges map of synthetic FLAIR, L1 = L1 loss, LEdge = L1 loss applied to edges map, LD = discriminator loss.

249x163mm (600 x 600 DPI)

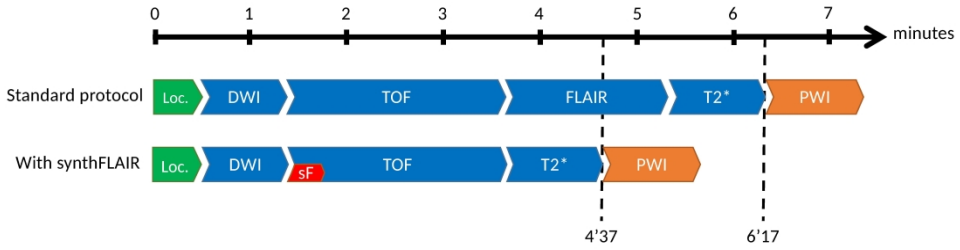

Supplemental Figure 2: Acquisition time reduction.
Duration of the latest stroke MR protocol in our institution is depicted. By removing real FLAIR acquisition and computing the synthetic FLAIR sequence during 3D TOF MR angiogram acquisition, the total duration would benefit from a 26% reduction, notwithstanding PWI. Loc. = localizer sequences, DWI = diffusion-weighted imaging, FLAIR = fluid-attenuated inversion recovery, TOF = time-of-flight angiogram, PWI = perfusion-weighted imaging, sF = synthetic FLAIR computation.

308x80mm (600 x 600 DPI)

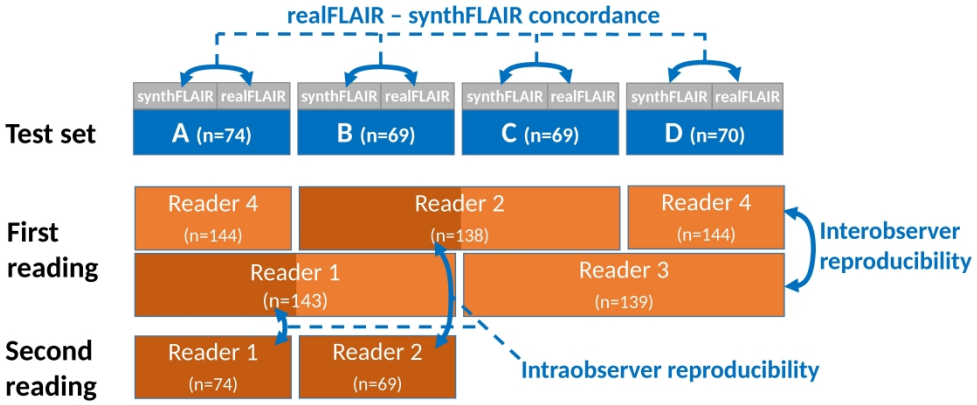

Supplemental Figure 3: FLAIR evaluation process.All patients in test set were evaluated by two distinct readers for interobserver reproducibility. Half of the test set was used for intraobserver reproducibility assessment. Concordance between real FLAIR and synthetic FLAIR was assessed first for each reader then after consensus. Number of MRI sets in each group is shown. FLAIR = fluid-attenuated inversion recovery, realFLAIR = real FLAIR, synthFLAIR = synthetic FLAIR

338x160mm (600 x 600 DPI)

Annex: List of studies with overlapping patients

Patient overlap number	Title	First Author	Journal	Year	DOI
44	MR imaging helps predict time from symptom onset in patients with acute stroke: implications for patients with unknown onset time	Petkova	Radiology	2010	10.1148/ radiol.10100461
115	Prevalence of MRI-defined recent silent ischemia and associated bleeding risk with thrombolysis	Tisserand	Neurology	2011	10.1212/ WNL.0b013e3182152855
176	Diffusion lesion reversal after thrombolysis: a MR correlate of early neurological improvement	Labeyrie	Stroke	2012	10.1161/ STROKEAHA.112.661009
186	Clinical and magnetic resonance imaging predictors of very early neurological response to intravenous thrombolysis in patients with middle cerebral artery occlusion	Apoil	J Am Heart Assoc	2013	10.1161/ JAHA.113.000511
330	Can DWI-ASPECTS substitute for lesion volume in acute stroke?	de Margerie-Mellon	Stroke	2013	10.1161/ STROKEAHA.113.003047
184	Clot burden score on admission T2*-MRI predicts recanalization in acute stroke	Legrand	Stroke	2013	10.1161/ STROKEAHA.113.001026
228	Magnetic Resonance Imaging-DRAGON score: 3-month outcome prediction after intravenous thrombolysis for anterior circulation stroke	Turc	Stroke	2013	10.1161/ STROKEAHA.111.000127
309	Mechanisms of unexplained neurological deterioration after intravenous thrombolysis	Tisserand	Stroke	2014	10.1161/ STROKEAHA.114.006745
30	Is white matter more prone to diffusion lesion reversal after thrombolysis?	Tisserand	Stroke	2014	10.1161/ STROKEAHA.113.004000
279	Unexplained early neurological deterioration after intravenous	Seners	Stroke	2014	10.1161/ STROKEAHA.114.005426

	thrombolysis: incidence, predictors, and associated factors				
153	Susceptibility vessel sign on T2* magnetic resonance imaging and recanalization results of mechanical thrombectomy with stent retrievers: a multicentre cohort study	Soize	Eur J Neurol	2015	10.1111/ ene.12693
155	How sustained is 24-hour diffusion-weighted imaging lesion reversal? Serial magnetic resonance imaging in a patient cohort thrombolyzed within 4.5 hours of stroke onset	Soize	Stroke	2015	10.1161/ STROKEAHA.114.008322
141	Do FLAIR vascular hyperintensities beyond the DWI lesion represent the ischemic penumbra?	Legrand	AJNR Am J Neuroradiol	2015	10.3174/ ajnr.A4088
453	Clinical Scales Do Not Reliably Identify Acute Ischemic Stroke Patients With Large-Artery Occlusion	Turc	Stroke	2016	10.1161/ STROKEAHA.116.013144
267	Does Diffusion Lesion Volume Above 70 mL Preclude Favorable Outcome Despite Post-Thrombolysis Recanalization?	Tisserand	Stroke	2016	10.1161/ STROKEAHA.115.012518
322	Comparison between voxel-based and subtraction methods for measuring diffusion-weighted imaging lesion growth after thrombolysis	Ben Hassen	Int J Stroke	2016	10.1177/ 1747493015616636
164	Fluid-Attenuated Inversion Recovery Vascular Hyperintensities-Diffusion-Weighted Imaging Mismatch Identifies Acute Stroke Patients Most Likely to Benefit From Recanalization	Legrand	Stroke	2016	10.1161/ STROKEAHA.115.010999
63	Can a 15-sec FLAIR replace conventional FLAIR sequence in stroke MR protocols?	Benzakoun	J Neuroradiol	2017	10.1016/ j.neurad.2016.11.001

120	Is Unexplained Early Neurological Deterioration After Intravenous Thrombolysis Associated With Thrombus Extension?	Seners	Stroke	2017	10.1161/ STROKEAHA.116.015414
244	Do Fluid-Attenuated Inversion Recovery Vascular Hyperintensities Represent Good Collaterals before Reperfusion Therapy?	Mahdjoub	AJNR Am J Neuroradiol	2018	10.3174/ajnr.A5431
138	White matter hyperintensity burden in patients with ischemic stroke treated with thrombectomy	Boulouis	Neurology	2019	10.1212/ WNL.0000000000008317
156	MT-DRAGON score for outcome prediction in acute ischemic stroke treated by mechanical thrombectomy within 8 hours	Ben Hassen	J Neurointerv Surg	2020	10.1136/ neurintsurg-2019-015105
33	Tissue no-reflow despite full recanalization following thrombectomy for anterior circulation stroke with proximal occlusion: A clinical study	Schiphorst	J Cereb Blood Flow Metab	2021	10.1177/ 0271678X20954929
127	Benefit of first-pass complete reperfusion in thrombectomy is mediated by limited infarct growth	Ben Hassen	Eur J Neurol	2021	10.1111/ ene.14490
394	Tissue outcome prediction in hyperacute Ischemic Stroke: comparison of machine learning models	Benzakoun	J Cereb Blood Flow Metab	2021	10.1177/ 0271678X211024371

Synthetic FLAIR as a substitute for FLAIR sequence in acute ischemic stroke

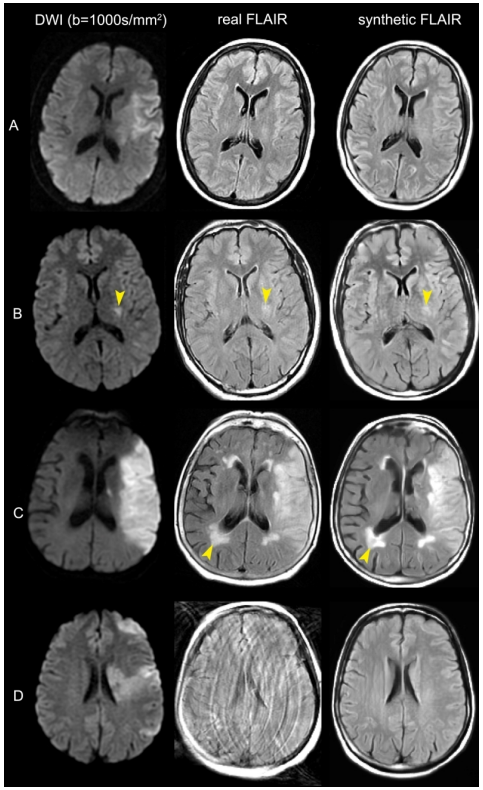

- Synthetic fluid-attenuated inversion recovery (FLAIR) can be generated from a diffusion-weighted imaging (DWI) sequence using deep learning within 22 seconds.
- The diagnostic performance of synthetic FLAIR to identify early (≤4.5hrs) ischemic stroke was similar to that of real FLAIR (sensitivity and specificity: 85% and 92% vs. 82% and 92%, respectively).
- Use of synthetic FLAIR instead of real FLAIR may allow a clinically relevant (≈25%) reduction in stroke MR protocol duration.

Benzakoun J et al. Published Online: DATE, 2021
https://doi.org/10.1148/radiol.2021211394